

RPS27 selectively regulates the expression and alternative splicing of inflammatory and immune response genes in thyroid cancer cells

Jing Wan^{1,B–D,F}, Juan Lv^{1,B,C}, Chun Wang^{2,B,C}, Li Zhang^{1,A,E,F}

¹ Ultrasound Department, People's Hospital of Xinjiang Uygur Autonomous Region, China

² Pathology Department, People's Hospital of Xinjiang Uygur Autonomous Region, China

A – research concept and design; B – collection and/or assembly of data; C – data analysis and interpretation;

D – writing the article; E – critical revision of the article; F – final approval of the article

Advances in Clinical and Experimental Medicine, ISSN 1899–5276 (print), ISSN 2451–2680 (online)

Adv Clin Exp Med. 2022;31(8):889–901

Address for correspondence

Li Zhang

E-mail: springwch@126.com

Funding sources

This research was funded by Natural Science Foundation of Xinjiang Uygur Autonomous Region (contract No. 2017D01C120). The funder had no role in study design, data collection and analysis, decision to publish, or preparation of the manuscript.

Conflict of interest

None declared

Received on August 16, 2021

Reviewed on October 7, 2021

Accepted on March 10, 2022

Published online on May 12, 2022

Cite as

Wan J, Lv J, Wang C, Zhang L. RPS27 selectively regulates the expression and alternative splicing of inflammatory and immune response genes in thyroid cancer cells.

Adv Clin Exp Med. 2022;31(8):889–901.

doi:10.17219/acem/147271

DOI

10.17219/acem/147271

Copyright

Copyright by Author(s)

This is an article distributed under the terms of the Creative Commons Attribution 3.0 Unported (CC BY 3.0) (<https://creativecommons.org/licenses/by/3.0/>)

Abstract

Background. The expression of ribosomal protein S27 (RPS27) is upregulated in multiple human malignancies. In thyroid cancer, the expression of RPS27 is associated with patient outcomes. However, the carcinogenic mechanisms of *RPS27* and functions of *RPS27* in the initiation and progression of thyroid cancer are still not clear.

Objectives. To investigate the carcinogenic mechanisms of *RPS27* and functions of *RPS27* in the initiation and progression of thyroid cancer.

Materials and methods. The *RPS27* gene was overexpressed in BTH101 cells and the influence on the level of gene expression and alternative splicing (AS) was then analyzed by comparing the transcriptomes of the overexpressing cells with the controls. The procedures included cloning and plasmid construction of *RPS27*, cell culture and transfection, evaluation of *RPS27* overexpression, library preparation and sequencing, RNA-Seq raw data clean and alignment, differentially expressed genes (DEGs) analysis, AS analysis, quantitative real-time polymerase chain reaction (qRT-PCR) validation of DEGs and AS events (ASEs), and functional enrichment analysis.

Results. The results demonstrated that *RPS27* could selectively regulate the expression of genes associated with autoimmune thyroid disease, inflammatory/immune response and AS of genes associated with TRIF-dependent toll-like receptor signaling pathway and apoptotic process. The genes in question are *BMP6*, *SERPINA3*, *IL17B*, *IL17RN*, *HLA-B*, *PF4*, *HLA-DOB*, *MADCAM1*, *HLA-DQA1*, *TPO*, *HLA-B*, *HLA-DQA1*, *HLA-DOB*, *HLA-C*, *KRT8*, *CFLAR*, *HMGAI1*, *CASP8*, *CCNH*, *UBE2D3*, and *MAPK9*, among others.

Conclusions. The *RPS27* selectively regulated the expression and alternative splicing of genes involved in inflammatory/immune response and TRIF-dependent toll-like receptor signaling pathway, which were tightly associated with the initiation and progression of thyroid cancer. These results extend our knowledge on the molecular functions of *RPS27* in thyroid cancer cells and have a potential value in thyroid cancer treatment.

Key words: gene expression, thyroid cancer, alternative splicing, ribosomal protein S27, overexpression

Background

Thyroid cancer is a common endocrine tumor with an increasing incidence worldwide.¹ The age-standardized incidence rate of thyroid cancer rose by 20% from 1990 to 2013.² In China, a recent investigation reported a rapidly increasing number of thyroid cancer cases.³ The immune system plays a crucial role in prevention of tumors, as well as in their initiation and progression.⁴ Some tumor types are strongly correlated with chronic infectious or inflammatory diseases, whereas others are not, but inflammatory components are present in most of human neoplastic lesions. Studies have demonstrated that thyroid cancer can be associated with thyroid autoimmunity, even if the exact mechanisms remain poorly elucidated.^{5,6}

Ribosomal protein S27 (RPS27), also known as metallopeptidyl isomerase-1 (MPS-1), is a multifunctional protein ubiquitously expressed in most of the human normal tissues and primarily located in the cytoplasm.⁷ It serves as an RNA-binding protein (RBP) and subsequently affects the translation and degradation of many mRNAs.⁸ In addition to translation-related functions, ribosomal proteins are also associated with plenty of biological process functions, including apoptosis, genomic stability, development, and cell proliferation.⁹ The expression of RPS27 is upregulated in multiple human malignancies, including liver, prostate, colon, stomach, and head and neck cancers.^{10–12} In thyroid cancer, the expression of RPS27 is associated with patient outcomes.¹³ However, the carcinogenic mechanisms of RPS27 and functions of RPS27 in the initiation and progression of thyroid cancer are still not clear.

Therefore, in this study, the *RPS27* gene was overexpressed in BTH101 cells and the influence on the gene expression level and alternative splicing (AS) was then analyzed through comparing the transcriptomes of the over-expressing cells with the controls.

Objectives

The objectives were to investigate the carcinogenic mechanisms of *RPS27* and functions of *RPS27* in the initiation and progression of thyroid cancer.

Materials and methods

Cloning and plasmid construction of RPS27

CE Design v. 1.04 (Vazyme Biotech, Nanjing, China) was employed to design the primer pairs for Hot Fusion. Each of the primers consists of a fragment of gene-specific sequence and a 17–30 bp sequence of the pIRES-hrGFP-1a vector:

F-primer: agcccgggcgatccgaattc
ATGCCTCTCGCAAAGGATCTC
R-primer: gtcaccttgtagctctcgag
GTGCTGCTTCCTCCTGAAGGA.

The pIRES-hrGFP-1a vector was digested with EcoRI and XhoI (New England Biolabs (NEB), Ipswich, USA) for 2–3 h at 37°C. The enzyme-digested vector was then run on 1.0% agarose gel and purified with the Qiagen column kit (Qiagen, Hilden, Germany). Total RNA was extracted from BHT101 cells with TRIzol (Ambion, Invitrogen, Carlsbad, USA). The purified RNA was reversely transcribed for cDNA with oligo dT primer. The inserted fragment was synthesized through polymerase chain reaction (PCR) amplification. The ClonExpress® II One Step Cloning Kit (Vazyme Biotech, Nanjing, China) was used to ligate the linearized vector digested with EcoRI and XhoI and PCR insert. Plasmids were introduced into *Escherichia coli* strain through chemical transformation. Cells were plated onto Luria broth (LB) agar plates containing 1 µL/mL ampicillin, and incubated overnight at 37°C. Colonies were screened through colony PCR (28 cycles) with universal primers located on the backbone vector. Sanger sequencing was used to verify the insert sequence.

Cell culture and transfection

Chinese Academy of Sciences Cell Bank (Shanghai, China) provided the human thyroid cancer cell line BHT101. The BHT101 cells were cultured with 5% CO₂ at 37°C in Dulbecco's modified Eagle's medium (DMEM) containing 10% fetal bovine serum (FBS), 100 µg/mL of streptomycin and 100 U/mL of penicillin. Lipofectamine 2000 (Invitrogen) was employed to conduct plasmid transfection of BHT101 cells following the manufacturer's protocol, and transfected cells were harvested after 48 h for quantitative real-time PCR (qRT-PCR) and western blot analysis. This study complied with the Declaration of Helsinki and the study protocol was approved by the Ethical Committee of People's Hospital of Xinjiang Uygur Autonomous Region, China (approval No. KY20180118148).

Evaluation of RPS27 overexpression

The evaluation of RPS27 overexpression was performed by means of qRT-PCR and western blot analysis, using glyceraldehyde-3-phosphate dehydrogenase (GAPDH) as the control. The synthesis of cDNA was conducted through standard procedures, and qRT-PCR was performed on the Bio-Rad S1000 Thermal Cycler (Bio-Rad, Hercules, USA) with Bestar SYBR Green RT-PCR Master Mix (DBI Bioscience, Shanghai, China). The primers of RPS27 were 5'-TCCTTCATCCCTCTCCAGAA-3' (forward) and 5'-GTAGGCTGGCAGAGGACAGT-3' (reverse), respectively; and the primers of GAPDH were 5'-CGGAGTCAACGGATTGGTCTGAT-3' (forward) and 5'-AGCCTTCTCCATGGTGGTGAAGAC-3' (reverse), respectively. The 2^{-ΔΔCt} method was employed to evaluate the relative expression level of RPS27. The paired Student's t-test was used to perform the comparison between RPS27-overexpressed cells and control cells.

For western blot analysis, to prepare the total cell lysates, RPS27-overexpressed and control BHT101 cells were lysed in radioimmunoprecipitation assay (RIPA) buffer, containing 150 mM NaCl, 50 mM Tris-HCl (pH 7.4), 0.1% sodium dodecyl sulfate (SDS), 1.0% deoxycholate, 1 mM ethylenediaminetetraacetic acid (EDTA), and 1% Triton X-100. The samples were centrifuged at $12,000 \times g$ for 5 min. The supernatants were analyzed using a 10% SDS polyacrylamide gel electrophoresis (SDS-PAGE) gel and then transferred onto a polyvinylidene difluoride (PVDF) membrane (Merck Millipore, Burlington, USA). The RPS27 was detected with a monoclonal Flag antibody (Sigma-Aldrich, St. Louis, USA) diluted in Tris-buffered saline with Tween 20 (TBST) (1:2000), and GAPDH (ABclonal Technology, Cumming Park, USA) was used as the loading control (1:2000).

Library preparation and sequencing

Total RNA extracted from BHT101 cells was purified using 2 phenol-chloroform treatments and then treated using RQ1 DNase (Promega, Madison, USA) to remove DNA. The Smartspec Plus (Bio-Rad) was employed to evaluate the quality and quantity of the purified RNA by measuring the absorbance at 260 nm/280 nm (A260/A280), and 1.5% agarose gel electrophoresis was used to verify the integrity of the RNA.

The VAHTS Stranded mRNA-seq Library Prep Kit (Vazyme Biotech) was used to perform RNA-seq library preparation with 1 μ g of the total RNA. Polyadenylated mRNAs were converted into double-stranded cDNAs after purification and fragmentation. The DNAs were then ligated to VAHTS RNA Adapters (Vazyme Biotech) following end repair and A tailing. Purified ligation products ranging from 200 bps to 500 bps were digested using heat-labile uracil-DNA glycosylase (UDG), and the single-stranded cDNA was amplified, purified, quantified, and stored at -80°C before high-throughput sequencing.

For high-throughput sequencing, the libraries were prepared according to the instructions of the manufacturer and applied to Illumina HiSeq X Ten system (Illumina, Inc., San Diego, USA) for 150 nt paired-end sequencing.

RNA-Seq raw data clean and alignment

Raw reads with more than 2-N bases in raw sequencing reads were excluded. FASTX-Toolkit v. 0.0.13 (http://hannonlab.cshl.edu/fastx_toolkit/index.html) was then used to trim adaptors and low-quality bases. The short reads with less than 16 nt were also discarded. After that, clean reads were aligned to the GRCh38 genome with tophat2,¹⁴ allowing 4 mismatches. Uniquely mapped reads were used for calculation of gene reads number and fragments per kilobase of transcript per million fragments mapped (FPKM).¹⁵

Alternative splicing analysis

As described previously, the ABL alternative splicing (ABLAs) pipeline was employed to define and quantify the alternative splicing events (ASEs) between the samples.¹⁶ Briefly, the detection of 10 types of ASEs was based on the splice junction reads, including exon skipping (ES), alternative 5' splice site (A5SS), alternative 3' splice site (A3SS), intron retention (IR), mutually exclusive exons (MXE), mutually exclusive 5'UTRs (5pMXE), mutually exclusive 3'UTRs (3pMXE), cassette exon, A3SS&ES, and A5SS&ES.

qRT-PCR validation of differentially expressed genes and ASEs

In order to elucidate the validity of the RNA-seq data, the qRT-PCR was conducted for some of the differentially expressed genes (DEGs). The information of primers was demonstrated in Supplementary File 1. Total RNA remaining from RNA-seq library preparation was used for qRT-PCR. The RNA was reversely transcribed into cDNA using a M-MLV Reverse Transcriptase (Vazyme Biotech). The qRT-PCR was conducted on the StepOne Real-Time PCR System using the SYBR Green PCR Reagents Kit (Yeasen, Shanghai, China). The qRT-PCR conditions consisted of denaturing at 95°C for 10 min, 40 cycles of denaturing at 95°C for 15 s, and annealing and extension at 60°C for 1 min. The qRT-PCR amplifications were performed in triplicate for each sample. The expression levels of all selected DEGs were normalized against that of GAPDH.

Meanwhile, a qRT-PCR assay was also conducted for alternative splicing event (ASE) validation. The primers used were also presented in Supplementary File 1. To detect alternative isoforms, we used a boundary-spanning primer for the sequence encompassing the junction of constitutive exon and alternative exon, as well as an opposing primer in a constitutive exon. The boundary-spanning primer of alternative exon was designed according to “model exon” to detect model splicing or “altered exon” to detect altered splicing.

Statistical analyses

The R Bioconductor package edgeR (<https://bioconductor.org/packages/release/bioc/html/edgeR.html>) was employed to screen out the DEGs whose expression levels were assessed using FPKM.¹⁷ A false discovery rate (FDR) <0.05 and fold change (FC) >2 or <0.5 were set as the cutoff criteria for identifying DEGs. The Student's t-test was performed to evaluate the significance of the ratio alteration of ASEs between RPS27-overexpressed and control cells. Regulated alternative splicing events (RASEs) were identified when $p \leq 0.05$. To sort out functional categories of DEGs, Gene Ontology (GO) terms and Kyoto

Encyclopedia of Genes and Genomes (KEGG) pathways were identified using KOBAS 2.0 server (<http://kobas.cbi.pku.edu.cn/>).¹⁸ The hypergeometric test and Benjamini–Hochberg FDR controlling procedure were employed to define the enrichment of each term. The expression levels of RPS27, selected DEGs and ASEs were compared using the Student's t-test. Significance was set at $p < 0.05$.

Results

RNA-seq data analysis

The qRT-PCR and western blot were used to evaluate the efficacy of RPS27 overexpression (Fig. 1A,B). Six cDNA libraries were constructed and then sequenced for paired-end reads of each sample. The average high-quality reads of these 6 samples was 78.47 ± 3.92 million (Supplementary File 2). Among these reads, 94.04–96.39% were aligned and about 89.14–94.42% were uniquely aligned when they were mapped onto the reference genome with TopHat 2 (Supplementary File 2). Robust expression results for 20,994 genes were obtained from RNA-seq data (Supplementary File 3). A correlation matrix was computed with FPKM values for all 20,994 genes according to the Pearson's correlation coefficient (Fig. 1C).

RPS27 overexpression in BHT101 cell selectively regulates the expression of inflammatory and immune response genes

A total of 1504 genes were differentially expressed, including 604 upregulated and 900 downregulated. Supplementary File 4 provides the details of all the DEGs. A volcano plot (Fig. 1D) demonstrated the DEGs regulated by RPS27 overexpression. Figure 1E shows the hierarchical clustering of DEGs in control and RPS27 overexpression samples. These results showed that RPS27 overexpression extensively regulated gene expression in BHT101 cells.

According to the cutoff criteria, the upregulated and downregulated DEGs were enriched in 44 and 112 GO terms, respectively (Supplementary Files 5 and 6). Interestingly, the upregulated genes in the biological process terms of the GO analysis were mainly associated with the inflammatory and immune response (Fig. 1F), including *BMP6*, *SERPINA3*, *IL17B*, *IL1RN*, *HLA-B*, *PF4*, *HLA-DOB*, *MADCAM1*, and *HLA-DQA1*. Conversely, the downregulated genes were primarily involved in mitosis and mitotic cell cycle.

When the corrected p-values of the KEGG pathways were set at <0.05 , the upregulated and downregulated DEGs were enriched in 166 and 211 pathways, respectively (Supplementary Files 7 and 8). Strikingly, the upregulated genes were primarily associated with autoimmune thyroid disease (Fig. 1G), including *TPO*, *HLA-B*,

HLA-DQA1, and *HLA-DOB*. In contrast, the downregulated genes were primarily associated with pathways in cancer, HTLV-I infection and regulation of actin cytoskeleton (Fig. 1G).

The expression of the DEGs involved in the inflammatory and immune response and angiogenesis was quantified using RNA sequencing data, including *BMP6*, *SERPINA3*, *IL17B*, *IL1RN*, *HLA-B*, *PF4*, *HLA-DOB*, *MADCAM1*, *HLA-DQA1*, and *TPO*. The results demonstrated that their expressions were significantly upregulated (Fig. 2). Among them, we selected *BMP6*, *HLA-B*, *HLA-DQA1*, *IL17B*, and *SERPINA3* for further qRT-PCR validation analysis. The PCR primers were demonstrated in Supplementary File 1. The qRT-PCR results were in agreement with the sequencing data (Fig. 3).

RPS27 regulates the alternative splicing of a large number of immune-response genes

Among the 66.7 ± 3.0 million uniquely mapped reads, 47.08–47.97% were junction reads (Supplementary File 2). Compared with the reference genome annotation through the use of the Tophat2 pipeline, there were 62.69% annotated exons (230,287 out of 367,321 annotated exons), 152,726 known splice junctions and 111,776 novel splice junctions.

There were 16,925 known ASEs in the model gene which was termed as the reference genome, and 45,772 novel ASEs excluding intron retention events (Supplementary Files 9 and 10).

A total of 735 RASEs were identified, including 401 upregulated and 334 downregulated (Supplementary Files 11 and 12). The RPS27-regulated ASEs mainly included the A5SS (157), A3SS (146), ES (120), and cassette exon (73) (Fig. 4A). These results implied that RPS27 overall regulated ASEs in BHT101 cell. The genes whose levels of AS and expression were both regulated by RPS27 were overlapped in order to determine whether the increase in ASEs could be attributed to altered transcription,¹⁹ and 3 such genes were identified (Fig. 4B), including *ITGA1*, *NPNT* and *MACF1*. This result suggested that AS and transcriptional regulation might be partially coupled.

Interestingly, among the genes regulated by RPS27-mediated AS, most were enriched in “viral reproduction”, “TRIF-dependent toll-like receptor signaling pathway” and “MyD88-independent toll-like receptor signaling pathway”, including *HLA-C*, *KRT8*, *CFLAR*, *HMGA1*, *CASP8*, *CCNH*, *UBE2D3*, and *MAPK9* (Fig. 4C). In contrast, enriched KEGG pathways ($p < 0.05$) mainly included those associated with “pyrimidine metabolism”, “purine metabolism” and “ribosome” (Fig. 4D).

The ASEs of the genes involved in thyroid cancer were quantified using RNA sequencing data, including *HLA-C*, *KRT8*, *CFLAR*, *HMGA1*, *CASP8*, *CCNH*, *UBE2D3*, and *MAPK9*. The results showed that they were significantly upregulated (Fig. 5). To validate the ASEs identified from

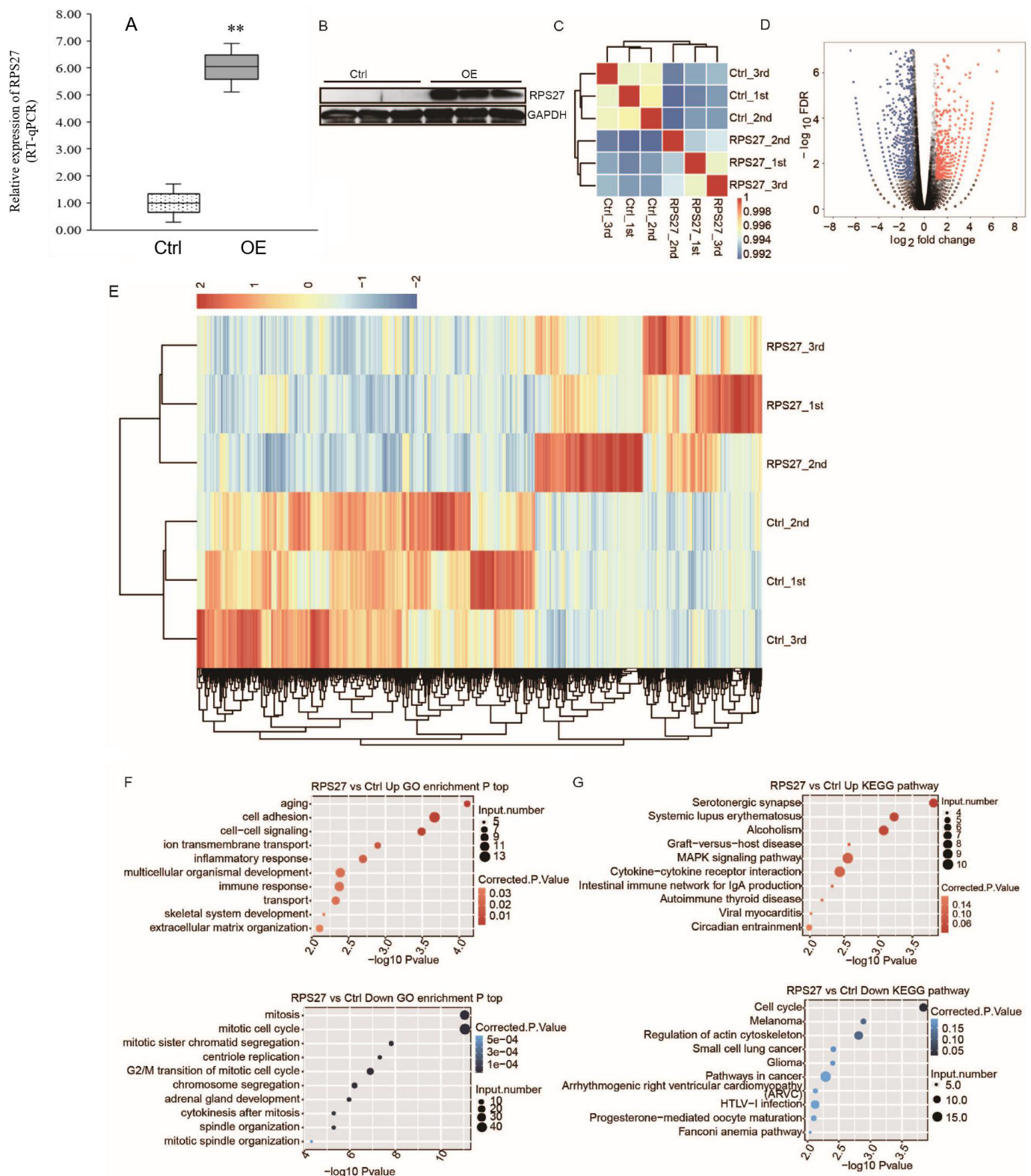


Fig. 1. RNA-seq analysis of ribosomal protein S27 (RPS27)-regulated transcriptome. A. RPS27 expression was quantified using quantitative real-time polymerase chain reaction (qRT-PCR); $t = -7.618$; $p = 0.002$; $**p < 0.01$; B. RPS27 expression was quantified using western blot; C. Heat map showing the hierarchically clustered Pearson's correlation matrix resulting from comparing the transcript expression values of the control cells with RPS27 overexpression cells; D. Identification of RPS27-regulated genes. Upregulated genes were labeled in red, whereas downregulated genes were labeled in blue in the volcano plot; E. Hierarchical clustering of differentially expressed genes (DEGs) in the control cells and RPS27 overexpression cells. Fragments per kilobase of transcript per million fragments mapped (FPKM) values were log₂-transformed and then median-centered by each gene; F. The top 10 representative Gene Ontology (GO) biological processes of up- or downregulated genes; G. The top 10 representative Kyoto Encyclopedia of Genes and Genomes (KEGG) pathways of up- or downregulated genes.

Control (Ctrl) – BHT101 cells without RPS27 overexpression; OE – BHT101 cells with RPS27 overexpression; GAPDH – glyceraldehyde-3-phosphate dehydrogenase; FDR – false discovery rate; IgA – immunoglobulin A.

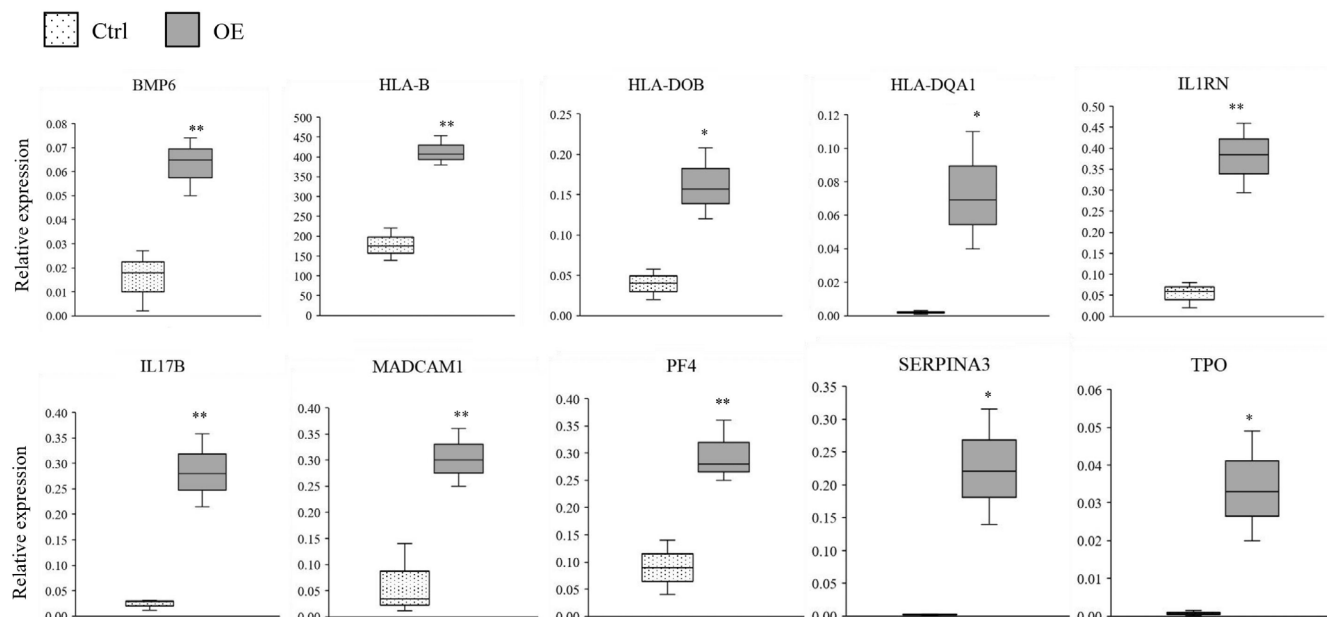


Fig. 2. Ribosomal protein S27 (RPS27) regulated the expression of the genes involved in the inflammatory and immune response and angiogenesis. Gene expression was quantified using RNA sequencing data. Fragments per kilobase of transcript per million fragments mapped (FPKM) values were calculated as explained in Materials and methods section; $t = -4.677, -7.468, -4.405, -3.495, -6.424, -6.243, -4.758, -4.727, -4.397, -3.955$; $p = 0.009, 0.002, 0.012, 0.025, 0.003, 0.003, 0.009, 0.009, 0.012, 0.017$; ** $p < 0.01$; * $p < 0.05$.

Control (Ctrl) – BHT101 cells without RPS27 overexpression; OE – BHT101 cells with RPS27 overexpression.

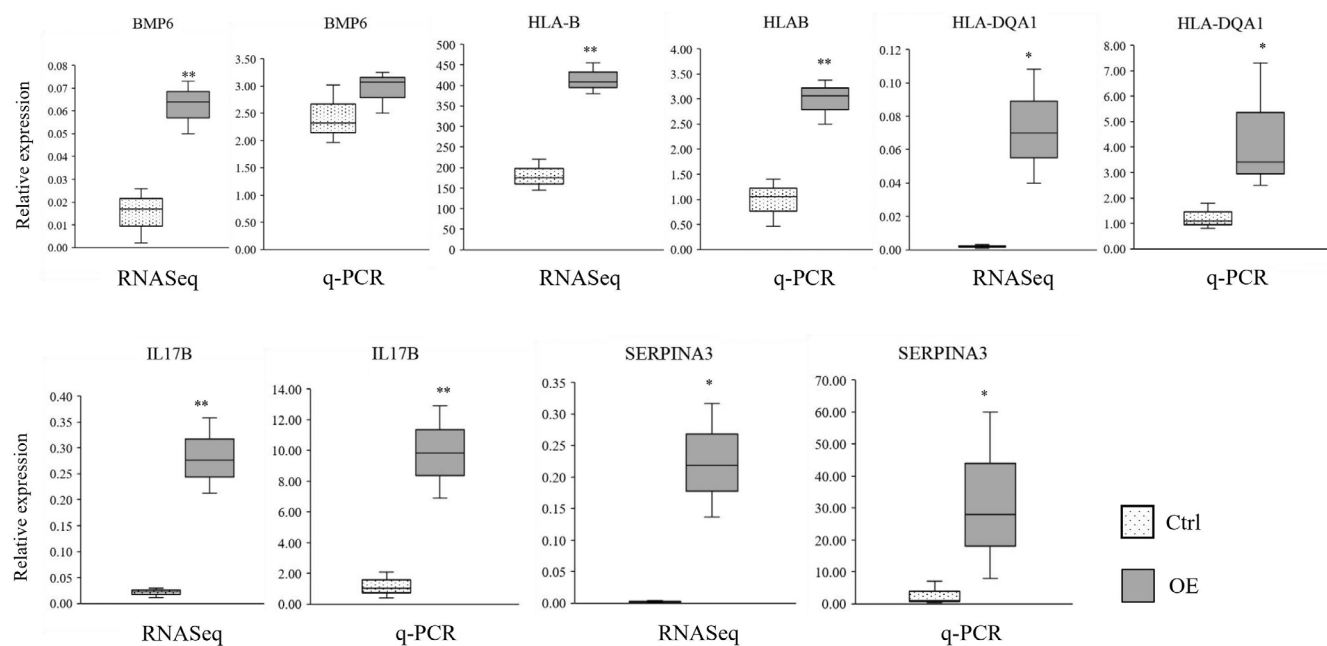


Fig. 3. Ribosomal protein S27 (RPS27) regulated the expression of *BMP6*, *HLA-B*, *HLA-DQA1*, *IL17B*, and *SERPINA3*. Both the RNA-seq and quantitative real-time polymerase chain reaction (qRT-PCR) validation are shown; $t = -4.677, -1.316, -7.468, -5.373, -3.495, -3.254, -6.243, -4.829, -4.397$; $p = 0.009, 0.259, 0.002, 0.006, 0.025, 0.026, 0.003, 0.008, 0.012$; $Z = -2.235$; $p = 0.043$; ** $p < 0.01$; * $p < 0.05$.

Control (Ctrl) – BHT101 cells without RPS27 overexpression; OE – BHT101 cells with RPS27 overexpression.

the RNA-Seq data, 4 potential ASEs were analyzed using qRT-PCR. They were located in *KRT8*, *CFLAR*, *CASP8*, and *CCNH* genes, respectively. The PCR primers were also demonstrated in Supplementary File 1. All the 4 ASEs validated with qRT-PCR were highly consistent with the sequencing results (Fig. 4E,F, Fig. 6).

Discussion

In this study, we profiled the entire transcriptome in BHT101 cells with the overexpression of RPS27, allowing for the decoding of RPS27-mediated regulation for gene expression and AS. Strikingly, the expression of genes

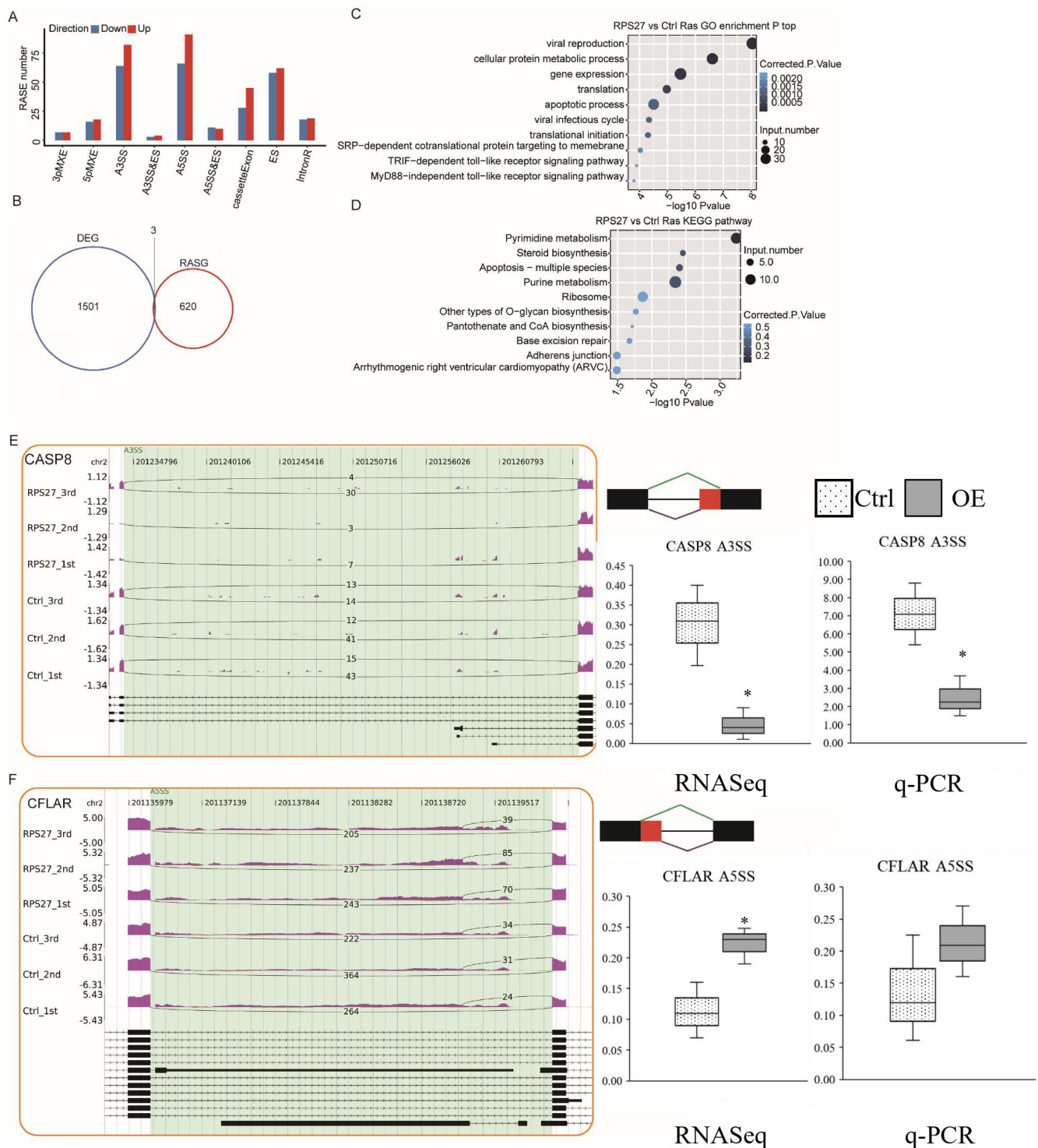


Fig. 4. Ribosomal protein S27 (RPS27) regulated alternative splicing events (ASEs) in BHT101 cells. **A.** Classification of RPS27-regulated ASEs; **B.** The overlap analysis between RPS27-regulated differentially expressed genes (DEGs) and alternative splicing genes (RASGs); **C.** The top 10 enriched Gene Ontology (GO) biological processes of RPS27-regulated alternative splicing genes; **D.** The top 10 enriched Kyoto Encyclopedia of Genes and Genomes (KEGG) pathways of RPS27-regulated alternative splicing (AS) genes; **E.** RPS27 regulated AS of CASP8, with IGV-Sashimi plot showing an alternative 3' splice sites (A3SS) event. Both RNA-seq quantification and quantitative real-time polymerase chain reaction (qRT-PCR) validation are presented; **F.** RPS27-regulated AS of CFLAR, with IGV-Sashimi plot showing an alternative 5' splice sites (A5SS) event. Both RNA-seq quantification and qRT-PCR validation are presented. Reads distribution of each ASE was plotted in the left panel with the transcripts of each gene shown below. The schematic diagrams depict the structures of ASEs, AS1 (purple line) and AS2 (green line). The constitutive exon sequences were denoted by black boxes, intron sequences by horizontal line (right panel, top), while alternative exon by red box and intron by purple box. The RNA-seq quantification is shown at the bottom of the right panel; $t = 4.406, 3.930, -3.058, -1.349$; $p = 0.016, 0.017, 0.025, 0.249$; $*p < 0.05$.

Control (Ctrl) – BHT101 cells without RPS27 overexpression; OE – BHT101 cells with RPS27 overexpression; 5pMXE – mutually exclusive 5'UTRs; 3pMXE – mutually exclusive 3'UTRs; ES – exon skipping.

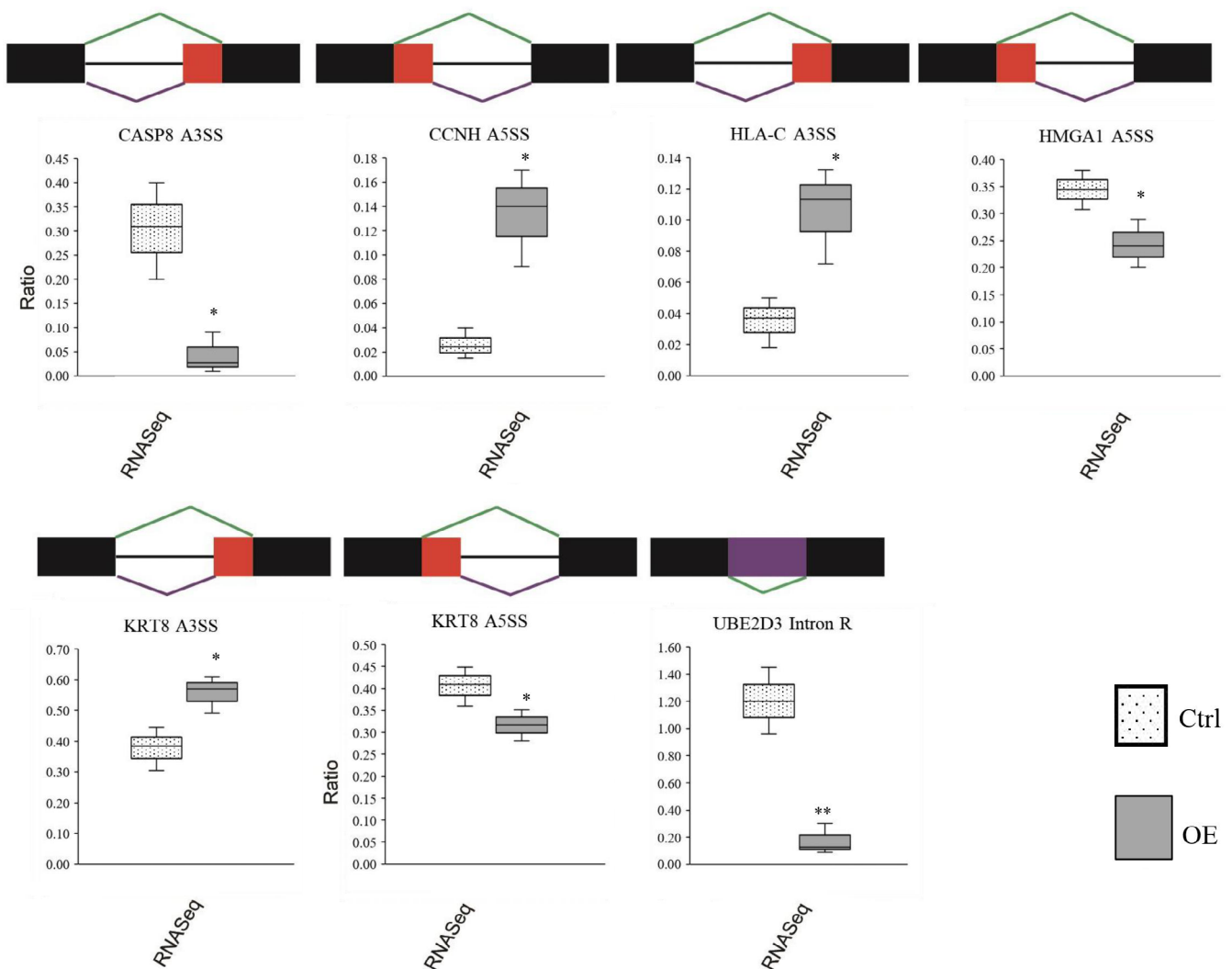


Fig. 5. Ribosomal protein S27 (RPS27) regulated alternative splicing (AS) of the genes associated with thyroid cancer, with alternative 3' splice sites (A3SS) for CASP8, alternative 5' splice sites (A5SS) for CCNH, A3SS for HLA-C, A5SS for HMGA1, A3SS for KRT8, A5SS for KRT8, and intron retention (IR) for UBE203. RNA-seq quantification is presented; $t = 4.159, -4.376, -3.534, 3.032, -3.337, 2.971, 6.627$; $p = 0.014, 0.012, 0.024, 0.039, 0.029, 0.042, 0.003$; ** $p < 0.01$; * $p < 0.05$.

Control (Ctrl) – BHT101 cells without RPS27 overexpression; OE – BHT101 cells with RPS27 overexpression.

involved in the inflammatory and immune response and autoimmune thyroid disease were selectively upregulated following RPS27 overexpression. Meanwhile, the genes whose AS was specifically regulated by RPS27 were enriched in the positive regulation of viral reproduction, apoptotic process, TRIF-dependent toll-like receptor signaling pathway, MyD88-independent toll-like receptor signaling pathway, and so forth. These results demonstrated that RPS27 was involved in the initiation and progression of thyroid cancer, possibly through regulating the expression of genes associated with autoimmune thyroid disease, and inflammatory and immune response and AS of genes associated with TRIF-dependent toll-like receptor signaling pathway and apoptotic process.

The upregulated genes associated with the inflammatory and immune response included *BMP6*, *SERPINA3*, *IL17B*, *IL1RN*, *HLA-B*, *PF4*, *HLA-DOB*, *MADCAM1*, and *HLA-DQA1*. Bone morphogenetic proteins (BMPs) are believed

to have complex roles in cancer progression.²⁰ Bentley et al. showed that BMP-6 was correlated with bone metastases in prostate cancer.²¹ Katsuta et al. found that a high expression of BMP6 was correlated with higher immune cell infiltration and better prognosis in estrogen receptor-positive breast cancer, whereas it was correlated with a worse prognosis in estrogen receptor-negative breast cancer.²² The expression of SERPINA3 has been detected in many tumor cells, including hepatocellular carcinoma, breast cancer, lung adenocarcinoma, and prostate cancer. Ko et al. indicated that SERPINA3 could promote hepatocellular carcinoma (HCC) cell survival and proliferation through upregulating the transcriptional activity of HNRNP-K.²³ Cao et al. demonstrated that the expression of SERPINA3 was higher in colon cancer tissues than in adjacent normal tissues, and silencing of SERPINA3 had significant effects on inhibiting the migration and invasion of colon cancer cells.²⁴ Recent studies have emphasized the potential role

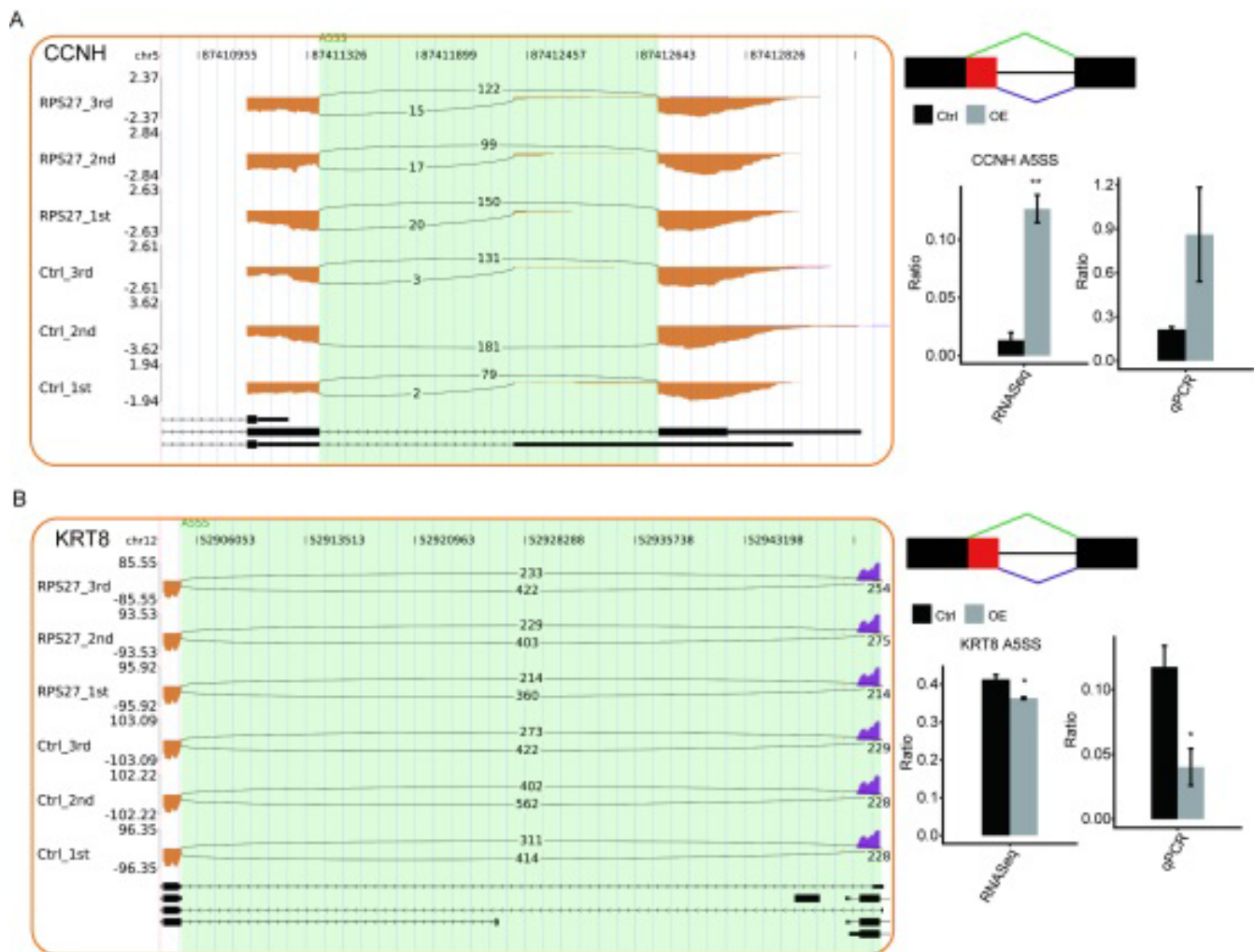


Fig. 6. Alternative splicing (AS) events of CCNH and KRT8 validated using quantitative real-time polymerase chain reaction (qRT-PCR) were highly consistent with the sequencing results

Control (Ctrl) – BHT101 cells without RPS27 overexpression; OE – BHT101 cells with RPS27 overexpression; A5SS – alternative 5' splice sites.

of the IL-17B/IL-RB pathway in cancer. The upregulated expression of IL-17B or its receptor has been correlated with a poor prognosis of various cancer types.^{25–27} In vitro cell assays demonstrate that IL-17B can promote the survival of breast cancer cells through enhancing the expression of anti-apoptotic Bcl-2 family members and activating the NF- κ B and ERK pathways.^{28,29} In thyroid cancer, IL-17B is confirmed to be able to promote the growth, invasion and migration of cancer cells in a dose-dependent manner.³⁰ The *IL1RN* (interleukin-1 receptor antagonist) gene plays a role in the pathogenesis of many autoimmune diseases. The *IL1RN*(VNTR) polymorphism may be correlated with susceptibility for Hashimoto's thyroiditis, a complex genetic autoimmune thyroid disease.³¹ The *IL1RN* polymorphisms are also associated with the susceptibility for cancers. Wang et al. found that *IL1RN* rs315919, rs452204 and rs3181052 polymorphisms were associated with a decreased risk of esophageal cancer in a Northwest Han Chinese population.³² Niedźwiecki et al. suggested that interleukin-1 receptor antagonist (IL-1ra) might have a critical

role in the development of anaplastic thyroid carcinoma and follicular thyroid carcinoma.³³ As a chemokine, platelet factor 4 (PF4, CXCL4) is involved in the pathogenesis of autoimmune thyroid diseases. Circulating PF4 levels are decreased in subclinically hypothyroid autoimmune thyroiditis (AIT).³⁴ Additionally, PF4 can regulate the inflammation within the tumor microenvironment, tumor angiogenesis, and, in turn, tumor growth.³⁵

The upregulated and downregulated DEGs were enriched in 166 and 211 pathways, respectively. Strikingly, the upregulated genes were associated with autoimmune thyroid disease, including *TPO*, *HLA-B*, *HLA-DQA1*, and *HLA-DOB*. The *TPO* plays a critical role in the production of thyroid hormones through catalyzing the iodination and coupling of tyrosyl residues to thyroglobulin.^{36,37} Many a study has investigated *TPO* as a marker for thyroid cancer. It is used as a thyroid differentiation marker,³⁶ and its expression is decreased in thyroid carcinoma.^{36,37} The human leukocyte antigen (*HLA*) gene is involved in the recognition and presentation of foreign antigens to the natural killer

cells (NK) and T lymphocytes, which is the starting point of the immune response.³⁸ This gene participates in tumor immunity and is a susceptibility gene for many cancers, including thyroid tumors.^{39,40} Some HLA alleles are risk factors for some tumors, whereas some have a protective role in tumorigenesis. Shuxian et al. showed that HLA-B*51:01 may be a susceptible allele for papillary thyroid carcinoma in the Chinese Han population of the Shandong coastal areas.⁴¹ The HLA-DQA1 is located on chromosome 6p21 and belongs to the MHC Class II family.⁴² It has a role in the progression of esophageal squamous-cell carcinoma (ESCC) and may be a biomarker for ESCC diagnosis and prognosis, as well as a potential target for the treatment of ESCC patients.⁴³ As the β -subunit of the HLA-DO class II paralogs, HLA-DOB has a negative regulation for major histocompatibility complex class II molecules through inhibiting HLA-DM molecules.⁴⁴ The DO:DM ratio defines major histocompatibility complex class II restricted-antigen presentation efficiency. Evidence has demonstrated that the dysregulation of the antigen presentation pathway has influence on development of cancer.⁴⁵ A report indicated that the single nucleotide polymorphism (SNP) of HLA-DOB rs2071554 was correlated with overall survival in patients with advanced non-small cell lung cancer treated with first-line chemotherapy.⁴⁶ Additionally, certain HLA-C alleles are also predisposing factors for papillary thyroid carcinoma.⁴⁷

Among the genes regulated by RPS27-mediated AS, some were enriched in “viral reproduction”, “TRIF-dependent toll-like receptor signaling pathway” and “MyD88-independent toll-like receptor signaling pathway”, including *HLA-C*, *KRT8*, *CFLAR*, *HMGA1*, *CASP8*, *CCNH*, *UBE2D3*, and *MAPK9*. Bromodomain-containing protein 4 (BRD4), belonging to the bromodomain and extra terminal domain family, has been reported to have important roles in various cancers. The abnormal expression of BRD4 is associated with tumor progression in thyroid cancer.⁴⁸ It can suppress tumor cell proliferation to inhibit the recruitment of BRD4 to the promoter complex of the *Ccnd1* and *Myc* genes in rat thyroid follicular PCCL3 cells.⁴⁹ In prostate cancer, the inhibition of BRD4 can suppress cell proliferation by regulating FOXO1-p21-Myc signaling.⁵⁰ In Merkel cell carcinoma, the disruption of BRD4 can inhibit MCC-3 xenograft tumor growth, possibly through downregulating c-Myc expression.⁵¹ Keratin8 (KRT8), the major component of the intermediate filament cytoskeleton, is correlated with progression and metastasis of several tumors. In gastric cancer, the abnormal expression of KRT8 can promote proliferation and migration of cancer cells through upregulating *MMP2*, *MMP9*, *PCNA*, and *TIMP1*.⁵² In lung adenocarcinoma, the expression of KRT8 is significantly elevated and may act as an independent prognostic factor for poor overall survival and recurrence-free survival.⁵³ In anaplastic thyroid carcinoma (ATC), the expression of KRT8 is upregulated, and upregulated KRT8 expression is critical for survival of ATC tumor

cells since siRNA-mediated knockdown of KRT8 expression leads to loss of cell viability and increased apoptosis in ATC-derived cells in vitro.⁵⁴ Mitogen-activated protein kinases (MAPKs) are associated with a large number of biological processes such as proliferation, differentiation, growth, migration, and apoptosis.⁵⁵ As a result, aberrant expression of MAPKs results in various diseases, including cancers.⁵⁶ The Mapk9, also named as JNK2, is a kinase from JNK subfamily. The function of JNK2 in cancers is still controversial. Several studies demonstrated that JNK2 acted as a tumor promoter in multiple myeloma, epidermal neoplasia, glioblastoma, breast cancer, and lung cancer.^{57–59} However, in bladder cancer and some lung and breast cancers, JNK2 appears to act as a suppressor.^{60,61} The high mobility group A1 (HMGA1) is an important member of superfamily of nonhistone chromatin binding proteins and plays a role in many cellular biology processes, such as embryogenesis, transcriptional regulation, viral integration, transformation, DNA repair, cell cycle regulation, and differentiation.⁶² The expression of HMGA1 is significantly upregulated in plenty of cancers, including thyroid, lung, colon, pancreas, breast, and ovary cancers.^{63–65} In addition, HMGA1 is confirmed to be correlated with high invasion and metastasis of thyroid cancer.^{65,66} The upregulated expression of HMGA1 can foster carcinogenesis and tumor progression via dysregulation of Wnt signaling and other developmental transcriptional networks.⁶⁷ Ubiquitin-conjugating enzyme E2D3 (UBE2D3) belongs to ubiquitin-conjugating enzyme (E2) family and is a critical component in ubiquitin (Ub) proteasome system (UPS).⁶⁸ Ubiquitin-dependent proteolysis by the 26S proteasome has a crucial role in the occurrence of tumors.⁶⁹ Guan et al. indicated that UBE2D3 might be a positive prognostic factor and might be associated with the expression of hTERT in esophageal cancer patients.⁷⁰ Additionally, the downregulation of UBE2D3 enhances radioresistance of esophageal cancer cells through prolonging IR-induced G2/M arrest and increasing telomere homeostasis,⁷¹ whereas its overexpression enhances radiosensitivity through degrading hTERT.⁷² Caspase 8 is an important component of the caspases family proteins that are the main regulatory and executive enzymes in the apoptosis pathway.⁷³ Apoptosis is associated with prevention from overproliferation in normal cells,⁷⁴ and the aberration of the apoptosis pathway is involved in the development of cancers.⁷⁵ Caspase 8 regulates the extrinsic apoptosis pathway,⁷⁶ and the *CASP8* -652 6N ins/del polymorphism is correlated with a decreased risk of various cancers.⁷⁷

The *CFLAR* gene encodes the apoptosis modulator protein c-FLIP, which has a critical role in regulating cell death.⁷⁸ One mechanism c-FLIP uses is forming heterodimers with caspase 8.⁷⁹ In HCC cells, the expression of *CFLAR* is significantly elevated, and the inhibition of *CFLAR* expression can reduce the proliferation of cancer cells.⁸⁰

In summary, the overexpression of RPS27 selectively regulated the expression and AS of inflammatory and immune response genes in thyroid cancer cells, whereas these genes had been confirmed to be involved in occurrence and development of cancer. Therefore, RPS27 was involved in the initiation and progression of thyroid cancer, possibly through regulating the expression of genes associated with autoimmune thyroid disease, and inflammatory and immune response and AS of genes associated with TRIF-dependent toll-like receptor signaling pathway and apoptotic process. These results broaden the current understanding on functions of RPS27 in the initiation and progression of thyroid cancer.

As for selection of cell lines, the objectives of this study were to investigate the carcinogenic mechanisms of RPS27 and functions of RPS27 in the initiation and progression of thyroid cancer, so selecting the normal cell line might not be enough. Meanwhile, we analyzed the expression of RPS27 in thyroid cancer through The Cancer Genome Atlas (TCGA). The results showed that the expression level of RPS27 in thyroid cancer tissues was not significantly different from normal tissues, but the upregulated expression of RPS27 in thyroid cancer tissues was associated with the prognosis of thyroid cancer patients. Therefore, we selected the BHT101 cells for this study.

Limitations

The limitations of this study mainly included 2 aspects. One aspect was that only a few DEGs and ASEs were validated through qRT-PCR, and the other aspect was that in vivo study was not performed.

Conclusions

THE RPS27 was involved in the initiation and progression of thyroid cancer, possibly through regulating the expression of genes associated with autoimmune thyroid disease and inflammatory and immune response, and the AS of genes associated with TRIF-dependent toll-like receptor signaling pathway and apoptotic process.

Data availability

The Supplementary Files are available at <https://doi.org/10.5281/zenodo.6324826>. The contents of the deposit are as follows:

Supplementary File 1. Primers used in qRT-PCR validation.

Supplementary File 2. Summary for RNA-seq reads used in this analysis.

Supplementary File 3. Robust expression results for 20,994 genes were obtained from RNA-seq data.

Supplementary File 4. The details of all the differentially expressed genes (DEGs).

Supplementary File 5. The upregulated differentially expressed genes (DEGs) were enriched in 44 GO terms.

Supplementary File 6. The downregulated differentially expressed genes (DEGs) were enriched in 112 Gene Ontology (GO) terms.

Supplementary File 7. The upregulated differentially expressed genes (DEGs) were enriched in 166 pathways.

Supplementary File 8. The downregulated differentially expressed genes (DEGs) were enriched in 211 pathways.

Supplementary File 9. There were 16,925 known alternative splicing events (ASEs) in the model gene which was termed as the reference genome.

Supplementary File 10. There were 45,772 novel alternative splicing events (ASEs) excluding intron retention events.


Supplementary File 11. Four hundred and one upregulated Regulated alternative splicing events (RASEs) were identified.

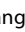
Supplementary File 12. Three hundred and thirty-four downregulated Regulated alternative splicing events (RASEs) were identified.

Supplementary File 13. Levene's test for equality of variances, Kolmogorov–Smirnov test and Student's t-test or Mann–Whitney U test.

ORCID iDs

Jing Wan  <https://orcid.org/0000-0002-3032-5047>

Juan Lv  <https://orcid.org/0000-0003-2758-4651>

Chun Wang  <https://orcid.org/0000-0002-0467-1093>

Li Zhang  <https://orcid.org/0000-0001-8541-0065>

References

- Harmer C. Foreword for special issue on thyroid cancer 2017. *Clin Oncol (R Coll Radiol)*. 2017;29(5):275. doi:10.1016/j.clon.2017.01.008
- Kim J, Gosnell JE, Roman SA. Geographic influences in the global rise of thyroid cancer. *Nat Rev Endocrinol*. 2020;16(1):17–29. doi:10.1038/s41574-019-0263-x
- Du L, Wang Y, Sun X, et al. Thyroid cancer: Trends in incidence, mortality and clinical-pathological patterns in Zhejiang province, South-east China. *BMC Cancer*. 2018;18(1):291. doi:10.1186/s12885-018-4081-7
- Galdiero MR, Varricchi G, Marone G. The immune network in thyroid cancer. *Oncoimmunology*. 2016;5(6):e1168556. doi:10.1080/2162402X.2016.1168556
- Ferrari SM, Fallahi P, Elia G, et al. Thyroid autoimmune disorders and cancer. *Semin Cancer Biol*. 2020;64:135–146. doi:10.1016/j.semcancer.2019.05.019
- Krátký J, Jiskra J. Autoimmune thyroiditis and thyroid cancer [in Czech]. *Vnitř Lek*. 2015;61(10):878–881. PMID:26486481.
- Feldheim J, Kessler AF, Schmitt D, et al. Ribosomal protein S27/metallopanstimulin-1 (RPS27) in glioma: A new disease biomarker? *Cancers (Basel)*. 2020;12(5):E1085. doi:10.3390/cancers12051085
- Revenkova E, Masson J, Koncz C, et al. Involvement of *Arabidopsis thaliana* ribosomal protein S27 in mRNA degradation triggered by genotoxic stress. *EMBO J*. 1999;18(2):490–499. doi:10.1093/emboj/18.2.490
- Zhou X, Liao WJ, Liao JM, et al. Ribosomal proteins: Functions beyond the ribosome. *J Mol Cell Biol*. 2015;7(2):92–104. doi:10.1093/jmcb/mjv014
- Atsuta Y, Aoki N, Sato K, et al. Identification of metallopanstimulin-1 as a member of a tumor associated antigen in patients with breast cancer. *Cancer Lett*. 2002;182(1):101–107. doi:10.1016/s0304-3835(02)00068-x
- Lee WJ, Keefer K, Hollenbeak CS, et al. A new assay to screen for head and neck squamous cell carcinoma using the tumor marker metallopanstimulin. *Otolaryngol Head Neck Surg*. 2004;131(4):466–471. doi:10.1016/j.otohns.2004.03.011

12. Wang YW, Qu Y, Li JF, et al. In vitro and in vivo evidence of metallopainstimulin-1 in gastric cancer progression and tumorigenicity. *Clin Cancer Res*. 2006;12(16):4965–4973. doi:10.1158/1078-0432.CCR-05-2316
13. Floristán A, Morales L, Hanniford D, et al. Functional analysis of RPS27 mutations and expression in melanoma. *Pigment Cell Melanoma Res*. 2020;33(3):466–479. doi:10.1111/pcmr.12841
14. Kim D, Pertea G, Trapnell C, et al. TopHat2: Accurate alignment of transcriptomes in the presence of insertions, deletions and gene fusions. *Genome Biol*. 2013;14(4):R36. doi:10.1186/gb-2013-14-4-r36
15. Trapnell C, Williams BA, Pertea G, et al. Transcript assembly and quantification by RNA-Seq reveals unannotated transcripts and isoform switching during cell differentiation. *Nat Biotechnol*. 2010;28(5):511–515. doi:10.1038/nbt.1621
16. Xia H, Chen D, Wu Q, et al. CELF1 preferentially binds to exon-intron boundary and regulates alternative splicing in HeLa cells. *Biochim Biophys Acta Gene Regul Mech*. 2017;1860(9):911–921. doi:10.1016/j.bbarm.2017.07.004
17. Robinson MD, McCarthy DJ, Smyth GK. edgeR: A bioconductor package for differential expression analysis of digital gene expression data. *Bioinformatics*. 2010;26(1):139–140. doi:10.1093/bioinformatics/btp616
18. Xie C, Mao X, Huang J, et al. KOBAS 2.0: A web server for annotation and identification of enriched pathways and diseases. *Nucleic Acids Res*. 2011;39(Web Server issue):W316–W322. doi:10.1093/nar/gkr483
19. Naftelberg S, Schor IE, Ast G, et al. Regulation of alternative splicing through coupling with transcription and chromatin structure. *Annu Rev Biochem*. 2015;84:165–198. doi:10.1146/annurev-biochem-060614-034242
20. Guo X, Wang XF. Signaling cross-talk between TGF- β /BMP and other pathways. *Cell Res*. 2009;19(1):71–88. doi:10.1038/cr.2008.302
21. Bentley H, Hamdy FC, Hart KA, et al. Expression of bone morphogenetic proteins in human prostatic adenocarcinoma and benign prostatic hyperplasia. *Br J Cancer*. 1992;66(6):1159–1163. doi:10.1038/bjc.1992.427
22. Katsuta E, Maawy AA, Yan L, et al. High expression of bone morphogenetic protein (BMP) 6 and BMP7 are associated with higher immune cell infiltration and better survival in estrogen receptor-positive breast cancer. *Oncol Rep*. 2019;42(4):1413–1421. doi:10.3892/or.2019.7275
23. Ko E, Kim JS, Bae JW, et al. SERPINA3 is a key modulator of HNRNP-K transcriptional activity against oxidative stress in HCC. *Redox Biol*. 2019;24:101217. doi:10.1016/j.redox.2019.101217
24. Cao LL, Pei XF, Qiao X, et al. SERPINA3 silencing inhibits the migration, invasion, and liver metastasis of colon cancer cells. *Dig Dis Sci*. 2018;63(9):2309–2319. doi:10.1007/s10620-018-5137-x
25. Yang YF, Lee YC, Lo S, et al. A positive feedback loop of IL-17B-IL-17RB activates ERK1/2 pathway to promote lung cancer metastasis. *Cancer Lett*. 2018;422:44–55. doi:10.1016/j.canlet.2018.02.037
26. Al-Samadi A, Moossavi S, Salem A, et al. Distinctive expression pattern of interleukin-17 cytokine family members in colorectal cancer. *Tumour Biol*. 2016;37(2):1609–1615. doi:10.1007/s13277-015-3941-x
27. Leivonen SK, Pollari M, Brück O, et al. T-cell inflamed tumor microenvironment predicts favorable prognosis in primary testicular lymphoma. *Haematologica*. 2019;104(2):338–346. doi:10.3324/haematol.2018.200105
28. Laprevotte E, Cochaud S, du Manoir S, et al. The IL-17B-IL-17 receptor B pathway promotes resistance to paclitaxel in breast tumors through activation of the ERK1/2 pathway. *Oncotarget*. 2017;8(69):113360–113372. doi:10.18632/oncotarget.23008
29. Huang CK, Yang CY, Jeng YM, et al. Autocrine/paracrine mechanism of interleukin-17B receptor promotes breast tumorigenesis through NF- κ B-mediated antiapoptotic pathway. *Oncogene*. 2014;33(23):2968–2977. doi:10.1038/ncr.2013.268
30. Ren L, Xu Y, Liu C, et al. IL-17RB enhances thyroid cancer cell invasion and metastasis via ERK1/2 pathway-mediated MMP-9 expression. *Mol Immunol*. 2017;90:126–135. doi:10.1016/j.molimm.2017.06.034
31. Zaaber I, Mestiri S, Marmouch H, et al. Polymorphisms in *TSHR* and *IL1RN* genes and the risk and prognosis of Hashimoto's thyroiditis. *Autoimmunity*. 2014;47(2):113–118. doi:10.3109/08916934.2013.866101
32. Wang T, Feng Y, Zhao Z, et al. IL1RN polymorphisms are associated with a decreased risk of esophageal cancer susceptibility in a Chinese population. *Chemotherapy*. 2019;64(1):28–35. doi:10.1159/000496400
33. Niedźwiecki S, Stepień T, Kuzdak K, et al. Serum levels of interleukin-1 receptor antagonist (IL-1ra) in thyroid cancer patients. *Langenbecks Arch Surg*. 2008;393(3):275–280. doi:10.1007/s00423-007-0251-9
34. Görar S, Ademoğlu E, Çarlıoğlu A, et al. Low levels of circulating platelet factor 4 (PF4, CXCL4) in subclinically hypothyroid autoimmune thyroiditis. *J Endocrinol Invest*. 2016;39(2):185–189. doi:10.1007/s40618-015-0348-x
35. Pilatova K, Greplova K, Demlova R, et al. Role of platelet chemokines, PF-4 and CTAP-III, in cancer biology. *J Hematol Oncol*. 2013;6:42. doi:10.1186/1756-8722-6-42
36. Caballero Y, López-Tomassetti EM, Favre J, et al. The value of thyroperoxidase as a prognostic factor for differentiated thyroid cancer: A long-term follow-up study. *Thyroid Res*. 2015;8:12. doi:10.1186/s13044-015-0022-6
37. Huang L, Wang X, Huang X, et al. Diagnostic significance of CK19, galectin-3, CD56, TPO and Ki67 expression and BRAF mutation in papillary thyroid carcinoma. *Oncol Lett*. 2018;15(4):4269–4277. doi:10.3892/ol.2018.7873
38. Robinson J, Halliwell JA, McWilliam H, et al. The IMGT/HLA database. *Nucleic Acids Res*. 2013;41(Database issue):D1222–D1227. doi:10.1093/nar/gks949
39. Ahn S, Choi HB, Kim TG. HLA and disease associations in Koreans. *Immune Netw*. 2011;11(6):324–335. doi:10.4110/in.2011.11.6.324
40. Amoli MM, Yazdani N, Amir P, et al. HLA-DR association in papillary thyroid carcinoma. *Dis Markers*. 2010;28(1):49–53. doi:10.3233/DMA-2010-0683
41. Shuxian J, Xiaoyun C, Zhihui F, et al. Association of HLA-B*51:01 with papillary thyroid carcinoma in the Chinese Han population of the Shandong coastal areas. *Thyroid*. 2014;24(5):867–871. doi:10.1089/thy.2013.0130
42. Wu C, Wang Z, Song X, et al. Joint analysis of three genome-wide association studies of esophageal squamous cell carcinoma in Chinese populations. *Nat Genet*. 2014;46(9):1001–1006. doi:10.1038/ng.3064
43. Shen FF, Pan Y, Li JZ, et al. High expression of HLA-DQA1 predicts poor outcome in patients with esophageal squamous cell carcinoma in Northern China. *Medicine (Baltimore)*. 2019;98(8):e14454. doi:10.1097/MD.00000000000014454
44. Denzin LK, Sant'Angelo DB, Hammond C, et al. Negative regulation by HLA-DO of MHC class II-restricted antigen processing. *Science*. 1997;278(5335):106–109. doi:10.1126/science.278.5335.106
45. Seliger B. Different regulation of MHC class I antigen processing components in human tumors. *J Immunotoxicol*. 2008;5(4):361–367. doi:10.1080/15476910802482870
46. Pu X, Hildebrandt MA, Lu C, et al. Inflammation-related genetic variations and survival in patients with advanced non-small cell lung cancer receiving first-line chemotherapy. *Clin Pharmacol Ther*. 2014;96(3):360–369. doi:10.1038/clpt.2014.89
47. Haghpanah V, Khalooghi K, Adabi K, et al. Associations between HLA-C alleles and papillary thyroid carcinoma. *Cancer Biomark*. 2009;5(1):19–22. doi:10.3233/CBM-2009-0564
48. Gao X, Wu X, Zhang X, et al. Inhibition of BRD4 suppresses tumor growth and enhances iodine uptake in thyroid cancer. *Biochem Biophys Res Commun*. 2016;469(3):679–685. doi:10.1016/j.bbrc.2015.12.008
49. Zhu X, Enomoto K, Zhao L, et al. Bromodomain and extraterminal protein inhibitor JQ1 suppresses thyroid tumor growth in a mouse model. *Clin Cancer Res*. 2017;23(2):430–440. doi:10.1158/1078-0432.CCR-16-0914
50. Tan Y, Wang L, Du Y, et al. Inhibition of BRD4 suppresses tumor growth in prostate cancer via the enhancement of FOXO1 expression. *Int J Oncol*. 2018;53(6):2503–2517. doi:10.3892/ijo.2018.4577
51. Sengupta D, Kannan A, Kern M, et al. Disruption of BRD4 at H3K27Ac-enriched enhancer region correlates with decreased c-Myc expression in Merkel cell carcinoma. *Epigenetics*. 2015;10(6):460–466. doi:10.1080/15592294.2015.1034416
52. Fang J, Wang H, Liu Y, et al. High KRT8 expression promotes tumor progression and metastasis of gastric cancer. *Cancer Sci*. 2017;108(2):178–186. doi:10.1111/cas.13120
53. Xie L, Dang Y, Guo J, et al. High KRT8 expression independently predicts poor prognosis for lung adenocarcinoma patients. *Genes (Basel)*. 2019;10(1):36. doi:10.3390/genes10010036
54. Guo D, Xu Q, Pabla S, et al. Cytokeratin-8 in anaplastic thyroid carcinoma: More than a simple structural cytoskeletal protein. *Int J Mol Sci*. 2018;19(2):577. doi:10.3390/ijms19020577

55. Dhillon AS, Hagan S, Rath O, et al. MAP kinase signalling pathways in cancer. *Oncogene*. 2007;26(22):3279–3290. doi:10.1038/sj.onc.1210421
56. Bubici C, Papa S. JNK signalling in cancer: In need of new, smarter therapeutic targets. *Br J Pharmacol*. 2014;171(1):24–37. doi:10.1111/bph.12432
57. Barbarulo A, Iansante V, Chaidos A, et al. Poly(ADP-ribose) polymerase family member 14 (PARP14) is a novel effector of the JNK2-dependent pro-survival signal in multiple myeloma. *Oncogene*. 2013;32(36):4231–4242. doi:10.1038/onc.2012.448
58. Nitta RT, Del Vecchio CA, Chu AH, et al. The role of the c-Jun N-terminal kinase 2- α -isoform in non-small cell lung carcinoma tumorigenesis. *Oncogene*. 2011;30(2):234–244. doi:10.1038/onc.2010.414
59. Cantrell MA, Ebelt ND, Pfefferle AD, et al. c-Jun N-terminal kinase 2 prevents luminal cell commitment in normal mammary glands and tumors by inhibiting p53/Notch1 and breast cancer gene 1 expression. *Oncotarget*. 2015;6(14):11863–11881. doi:10.18632/oncotarget.3787
60. Cellurale C, Weston CR, Reilly J, et al. Role of JNK in a Trp53-dependent mouse model of breast cancer. *PLoS One*. 2010;5(8):e12469. doi:10.1371/journal.pone.0012469
61. Pan CW, Liu H, Zhao Y, et al. JNK2 downregulation promotes tumorigenesis and chemoresistance by decreasing p53 stability in bladder cancer. *Oncotarget*. 2016;7(23):35119–35131. doi:10.18632/oncotarget.9046
62. Resar LM. The high mobility group A1 gene: Transforming inflammatory signals into cancer? *Cancer Res*. 2010;70(2):436–439. doi:10.1158/0008-5472.CAN-09-1212
63. Shah SN, Cope L, Poh W, et al. HMGA1: A master regulator of tumor progression in triple-negative breast cancer cells. *PLoS One*. 2013;8(5):e63419. doi:10.1371/journal.pone.0063419
64. Belton A, Gabrovsky A, Bae YK, et al. HMGA1 induces intestinal polypsis in transgenic mice and drives tumor progression and stem cell properties in colon cancer cells. *PLoS One*. 2012;7(1):e30034. doi:10.1371/journal.pone.0030034
65. Chiappetta G, Tallini G, De Biasio MC, et al. Detection of high mobility group I HMGI(Y) protein in the diagnosis of thyroid tumors: HMGI(Y) expression represents a potential diagnostic indicator of carcinoma. *Cancer Res*. 1998;58(18):4193–4198. PMID:9751634.
66. Zhong J, Liu C, Zhang QH, et al. TGF- β 1 induces HMGA1 expression: The role of HMGA1 in thyroid cancer proliferation and invasion. *Int J Oncol*. 2017;50(5):1567–1578. doi:10.3892/ijo.2017.3958
67. Resar L, Chia L, Xian L. Lessons from the crypt: HMGA1-amping up Wnt for stem cells and tumor progression. *Cancer Res*. 2018;78(8):1890–1897. doi:10.1158/0008-5472.CAN-17-3045
68. Wu K, Kovacev J, Pan ZQ. Priming and extending: A UbcH5/Cdc34 E2 handoff mechanism for polyubiquitination on a SCF substrate. *Mol Cell*. 2010;37(6):784–796. doi:10.1016/j.molcel.2010.02.025
69. Kraus WE, Muoio DM, Stevens R, et al. Metabolomic quantitative trait loci (mQTL) mapping implicates the ubiquitin proteasome system in cardiovascular disease pathogenesis. *PLoS Genet*. 2015;11(11):e1005553. doi:10.1371/journal.pgen.1005553
70. Guan GG, Wang WB, Lei BX, et al. UBE2D3 is a positive prognostic factor and is negatively correlated with hTERT expression in esophageal cancer. *Oncol Lett*. 2015;9(4):1567–1574. doi:10.3892/ol.2015.2926
71. Yang H, Wu L, Ke S, et al. Downregulation of ubiquitin-conjugating enzyme UBE2D3 promotes telomere maintenance and radioresistance of Eca-109 human esophageal carcinoma cells. *J Cancer*. 2016;7(9):1152–1162. doi:10.7150/jca.14745
72. Gao X, Wang W, Yang H, et al. UBE2D3 gene overexpression increases radiosensitivity of EC109 esophageal cancer cells in vitro and in vivo. *Oncotarget*. 2016;7(22):32543–32553. doi:10.18632/oncotarget.8869
73. Yu J, Zhang L, Hwang PM, et al. PUMA induces the rapid apoptosis of colorectal cancer cells. *Mol Cell*. 2001;7(3):673–682. doi:10.1016/s1097-2765(01)00213-1
74. Hengartner MO. The biochemistry of apoptosis. *Nature*. 2000;407(6805):770–776. doi:10.1038/35037710
75. Thompson CB. Apoptosis in the pathogenesis and treatment of disease. *Science*. 1995;267(5203):1456–1462. doi:10.1126/science.7878464
76. Tummers B, Green DR. Caspase-8: Regulating life and death. *Immunol Rev*. 2017;277(1):76–89. doi:10.1111/imr.12541
77. Cai J, Ye Q, Luo S, et al. CASP8-652 6N insertion/deletion polymorphism and overall cancer risk: Evidence from 49 studies. *Oncotarget*. 2017;8(34):56780–56790. doi:10.18632/oncotarget.18187
78. Faiz A, Heijink IH, Vermeulen CJ, et al. Cigarette smoke exposure decreases CFLAR expression in the bronchial epithelium, augmenting susceptibility for lung epithelial cell death and DAMP release. *Sci Rep*. 2018;8(1):12426. doi:10.1038/s41598-018-30602-7
79. Ueffing N, Singh KK, Christians A, et al. A single nucleotide polymorphism determines protein isoform production of the human c-FLIP protein. *Blood*. 2009;114(3):572–579. doi:10.1182/blood-2009-02-204230
80. Wang Y, Zhao YR, Zhang AY, et al. Targeting of miR-20a against CFLAR to potentiate TRAIL-induced apoptotic sensitivity in HepG2 cells. *Eur Rev Med Pharmacol Sci*. 2017;21(9):2087–2097. PMID:28537677.